Probabilistic Assessment of PGA and UHS for Bojnurd city, the Capital of North Khorasan Province, Iran

Mohammad Ali Rahgozar[1*], Gholamreza Ghodrati Amiri [2], and Mansour Saleh[3]

1.Assistant Prof., Department of Civil Engineering, Faculty of Engineering, University of Isfahan, Isfahan, Iran, * Corresponding Author; email: rahgozar@eng.ui.ac.ir
2. Prof., Center of Excellence for Fundamental Studies in Structural Engineering, College of Civil Engineering, Iran University of Science & Technology, Tehran, Iran
3. Research Fellow, Department of Civil Engineering, Azad University, Shahrekord Branch, Shahrekord, Iran

Received: 03/01/2012
Accepted: 19/06/2012

ABSTRACT

Probabilistic seismic hazard assessment (PSHA) of horizontal peak ground acceleration (PGA) and Uniform Hazard Spectra (UHS) on bedrock for different hazard levels is conducted in this study for Bojnurd city, the capital of North Khorasan province, Iran. Therefore, all historical and instrumental earthquakes in a radius of 200 km of the center of Bojnurd city are gathered and after elimination of the aftershocks and foreshocks, the main earthquakes are identified in order to calculate the seismic parameters by Kijko (2000) method. The seismotectonic model of the considered region and the seismic sources of the region have been modeled. Bojnurd city and its vicinity are meshed by 8 vertical and 11 horizontal lines. PGAs and UHS are calculated for all 88 points of the mesh using the logic tree method and different attenuation relationships with different weighted coefficients. These calculations are performed for two hazard levels of 10% and 2% probability of being exceeded in 50 years (hazard levels 1 and 2 respectively). Regional seismic hazard maps for PGAs and UHS for different locations of Bojnurd city and its vicinity are provided.

Keywords:
Probabilistic seismic hazard assessment; Seismicity parameters; Peak ground acceleration; Uniform hazard spectra; Bojnurd; Iran

1. Introduction

Bojnurd (or Bojnord) is the capital of North Khorasan province in the northeast of Iran. This study intends to provide a comprehensive probabilistic seismic assessment of Bojnurd city and its surrounding area encircling a radius of 200 km from the center of Bojnurd city. North Khorasan province situated between latitudes of 36° 42' to 38° 14' N and longitudes of 56° 3' to 58° 3' E. Its neighbors are: the country of Turkmenistan (with a border of 270 km) from north, Razavi Khorasan from east and south, Semnan province from southwest, and Golestan province from west. Bojnurd is 701 km away from Tehran [1].

Due to historical, cultural and industrial importance of the city of Bojnurd, as well as its many other potentialities for development, it is becoming one of the significant centers of the country. Any strong earthquake may then cause considerable damages to it. Therefore, the importance of a probabilistic seismic hazard study for this city is obvious.

Active faulting in Iran is a direct indicator of active crustal deformation due to the convergence between Arabia and Eurasia, see Figure (1). According to Hessami and Jamali [2] in terms of seismicity and active faulting, Iranian plateau can be described as follows: Active faults in Zagros are blind and the focal mechanism solutions of the earthquakes of the region point to the presence of both thrust and

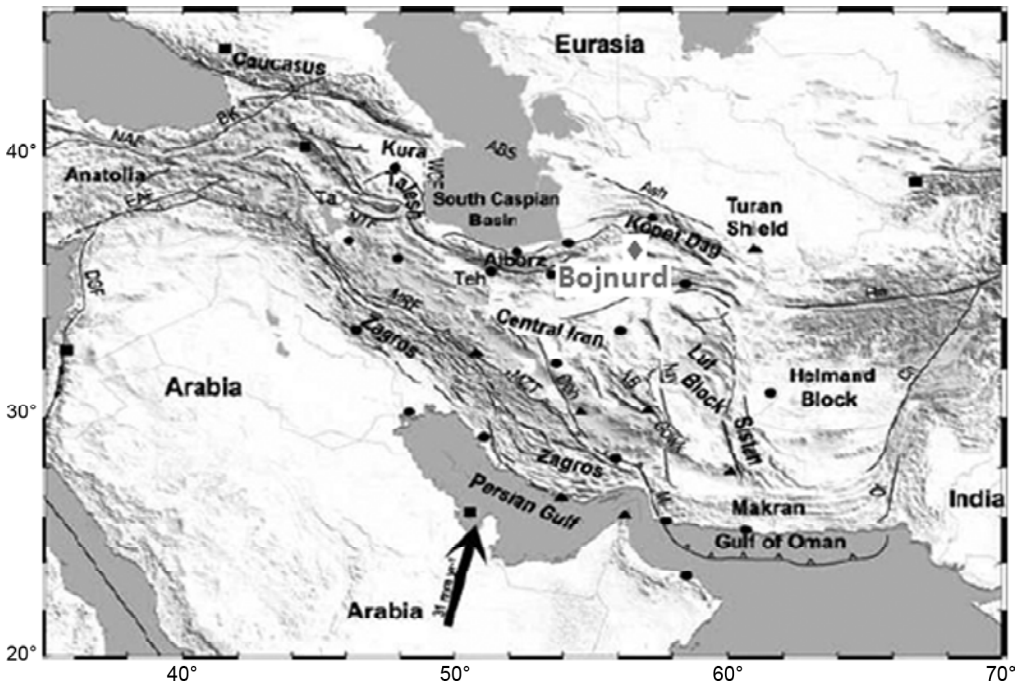

Figure 1. Seismotectonic map of major active faults in Iranian plateau [6].

transverse strike slip faulting in its basement. Whereas in the rest of the country, most active faults reach the surface. The earthquake mechanism solutions along active fault systems in eastern and central Iran imply dominance of strike-slip faulting in a transpression regime. Conversely, active faults in NW Iran are transtensive. The Alborz and Kopeh-Dagh fault zones are relatively vast active fault zones in which the locating of individual active faults is difficult. In the south east, the Makran fault has raised terraces in the shores of the Oman Sea, and caused many earthquakes and tsunamis in the region [3]. Central Iran, on the other hand, is not very active seismically.

Based on some geological, geophysical and seismological similarities and the assumption of uniform earthquake potential, Tavakoli [4] has divided Iran into 20 seismotectonic provinces. The active faults are located in parts of these twenty known seismotectonic provinces, see Figure (2). An area bounded by geological features marks a difference in seismic characteristics of one province from its neighboring provinces. Each province has equal seismic potential and uniform geological structure and trends. This map is obtained based on a catalogue of large and damaging Iranian earthquakes for the correlation between seismic activity and seismotectonic provinces. The boundaries of the provinces are established through analysis of seismic history, relocated epicenter for the past several decades, tectonic environments, active faults, regional geomorphology, and plate boundaries [4].

The geographic coordinates of the center of Bojnurd city are 37°28'30"N and 57°20'00"E. Based on geological and geotectonical references, Bojnurd region, defined as above, is situated in the 14th and mainly in the 19th provinces (zones of Eastern Alborz and Kopeh-Dagh belts, respectively, see Figure (2) [4]. Occurrence of several earthquakes in recent years in the region (especially since 2000)

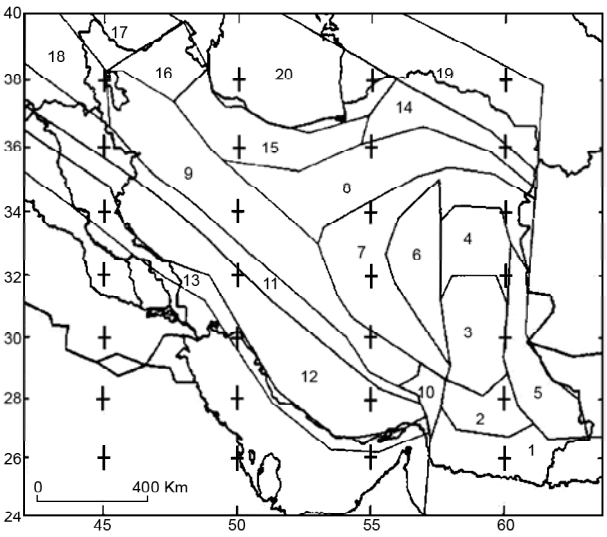

Figure 2. Iran seismotectonic provinces [2].

proves that the faults of Alborz and mainly on Kopeh-Dagh belts have been activated [5-6].

The main contribution of this research is intended to be the derivation of site specific UHS and PGA for different hazard levels for the first time for the city of Bojnurd. The city of Bojnurd by recently becoming the capital of North Khorasan province and its potential for a rapid future expansion is in great need of the outcome of such researches. The latest available information on different probabilistic assessment methodologies, attenuation relationships, and seismic source zones in the region, etc. has led to a more realistic assessment of the seismic risks in the studied region. In fact, Iran's seismic code authorities have now got higher responsibility to expand such studies for the entire country.

2. Importance of Uniform Hazard Spectra

Most of the modern seismic design codes are now switched to directly using Uniform Hazard Spectra (UHS) rather than relying on the design spectra obtained from peak ground motion bounds. The derivation of spectral shapes from peak ground motion bounds is based on studies carried out by Newmark and Hall [7]. In these studies, the spectral shapes were obtained by averaging the spectral curves for ground motion records from a few earthquakes. Most of these earthquakes were in the magnitude range of 6 to 7 with a distance-to-the-source of about 20 km. It is now recognized that the idealized spectrum derived as above may deviate significantly from the true spectrum for a site, and the error can be as large as 300% [8]. Spectral shape for a site is governed by the magnitudes and source distances of earthquakes that contribute most significantly to the hazard. If, for a given site, these parameters are different from those used in deriving the standard spectral shapes, the site-specific spectra deviate considerably from the standard spectra. Since the mid-1970s, methodologies have become available for deriving linear elastic spectra for a given site and for a given "uniform" hazard level, say 2 or 10% probability of being exceeded in 50 years, for the entire period range. Such spectra are called uniform hazard spectra (UHS). They provide spectral accelerations at specified values of the period of an elastic single-degree-of-freedom (SDOF) system. Because UHS provides response parameters that can be used directly in estimating the design earthquake forces, they are preferable to the spectra derived indirectly from peak ground motion bounds.

Unfortunately, the seismic design code of Iran, Std. 2800 still relies on design spectra based on peak ground acceleration, PGA or A as it is called in that standard [9]. This study attempts to provide iso-response acceleration zoning maps of the studied region both in terms of PGA, and UHS entire period range.

3. Geology and Tectonics of the Studied Region

The studied region includes two main active seismic zones of Iranian plateau, namely Eastern Alborz and Kopeh-Dagh in the 14th and 19th provinces, respectively, see Figure (2) [4].

3.1. Kopeh-Dagh

It is referred to as "Kopeh-Dagh" after its highest structure, the Kopeh-Dagh mountain range, see Figure (1). Structurally, it represents the margin of Central Iran at the edge of the Turan Plate. It constitutes the northeastern limit of the Alpine-Himalayan mountain belt, and, in this respect, it is a structure homologous to the Zagros which forms the corresponding southwestern limit, see Figure (1). The main structural units are: the Turan Plate, the Main Fault Zone, the Kopeh-Dagh range, the Atrek-Kashaf Lineament, the Allah Dagh-Binalud range and Central Iran. The Kopeh-Dagh and Allah Dagh-Binalud mountain ranges together form a mountain belt about 600 km long and up to 200 km wide. They represent thicknesses of up to 10 km of Mesozoic and Tertiary sediments which, during the last phase of the Alpine orogeny, were folded into long linear folds concave in plan towards the south. Maximum heights are over 3000 m, contrasting sharply with the near uniform 100 m altitude of the Turan Plate. The Allah Dagh-Binalud range is the eastern continuation of the Alborz range of North central Iran and dates from the Paleogene-Neogene, whereas the Kopeh-Dagh range was formed later during the Neogene-Quaternary [10]. The mountains are highest and narrowest in the center and east, and relatively lower in the west, a morphological contrast to an "uplifted" Central and Eastern Kopeh-Dagh from a "subsided" Western Kopeh-Dagh. In the northeast, the Kopeh-Dagh range is limited by the Main Fault Zone, which truncates the folds in the

west but is parallel to them in the east. This fault zone corresponds to a fundamental basement structure separating the Turan Plate from the Kopeh-Dagh. At the surface, it is located between narrow box-like folds of a frontal range (the Peredovoy range) in the south, and a narrow longitudinal foothill basin (the "Foredeep") in the north. The Main Fault Zone is formed by three partly overlapping fault segments parallel to the overall NW structure and each slightly offset with respect to the other. The regions of overlap are characterized by short south-dipping folds and thrusts striking on average east-west. Each fault segment at its south-eastern end bends into a NNW-SSE fault zone which extends into the mountain range and in some cases bends into fault zones passing near cities like Bojnurd and Quchan. The narrow NW-SE basin separating the Kopeh-Dagh from the Allah Dagh-Binalud ranges is approximately parallel to the Main Fault Zone, and is also generally thought to correspond to a basement structure. The southern limit of the Allah Dagh-Binalud range is not defined by any single structure comparable to the Main Fault Zone. The geomorphological limit appears to be the longitudinal basin extending from Neyshabur in the east to Esfarayan and Shahrud in the west. In the west, the coastal lowlands adjoining the Caspian Sea limit the Kopeh-Dagh near 55° E. Subsidence has been proceeding here, probably along meridional basement step-faults, since the end of the Pliocene. Farther south, however, the Allah Dagh is continued by the Alborz, which bends around the southern Caspian Sea. In the east, the limits of the region are taken here at longitude 60° E, beyond which there occurs a very sudden decrease in seismicity. The corresponding structure is associated with a northern continuation of the East Iranian Rift described in the Lut region farther south, and with a north-south basement structure often postulated in the Turan Plate [11].

The region considered under the general term 'Kopeh-Dagh' is located east of the Caspian Sea, and includes Northeast Iran and southern Turkmenistan. The seismicity of the region over the last 100 years, according to Tchalenko [11]), indicates that the major earthquakes were located on the NNW-SSE "Bakharden-Quchan Zone", which forms part of the Diagonal Fault System. The 1929 Baghan-Germab (M_S = 7.3) earthquake, in particular, was accompanied by a surface fracture over 50 km long caused by re-activation of one of the faults of this Zone. The overall seismotectonics of the Kopeh-Dagh is interpreted in terms of an eastern "NNW trend" which is separated by a longitudinal zone of relative quiescence near 56-57° E from a western "NNE trend". Active surface structures throughout the region are on average consistent with a tectonic model based on a NNE motion of Iran with respect to the Turan Plate [11].

In Kopeh-Dagh, a region in northeast of Iran, strike slip faults form conjugate shear faults. The north-northwestern trending faults are dominant in the eastern Kopeh-Dagh. The 1929/5/1 Baghan-Germab earthquake is the only earthquake in Kopeh-Dagh which is associated with surface faulting [2]. The surface rupture associated with the Baghan-Germab earthquake has a north-northwestern trend and a length of 50 km to 70 km [2]. Ambraseys and Melville report an oblique motion (right-lateral and reverse movement) on this fault. Movement on the faults with northeastern trends indicates a combination of left-lateral strike slip and normal components. The focal mechanism solutions of the 1970/7/30 and 1974/3/7 earthquakes in western Kopeh-Dagh indicate domination of left-lateral strike slip movement with a small normal component on northeastern nodal planes [40]. The northeastern boundary of Kopeh-Dagh is marked by the Main Kopeh-Dagh fault. Although the measured displacement by Trifonov [66] suggests a right-lateral strike slip movement on this fault, the solution of the focal mechanism for the 1948/10/5 Ashkhabad earthquake on this fault zone indicates thrust faulting with a southwestern dip direction. On the southern margin of Kopeh-Dagh, activity of Esfarayen thrust has been documented by the 1969/1/3 earthquake. Recent activity of Kashafrud and Quchan faults within Kopeh-Dagh has also been documented [2].

3.2. Alborz

The Alborz region is an active zone with a high density of active faults. Since many of the region's earthquakes were not associated with surface faulting, and the meizoseismal areas of many of these earthquakes are relatively large, locating the active fault becomes complicated. The most important faults in the southern edge of Alborz, which their activity has been documented using both seismicity and field investigations, are: The North Tehran fault, Mosha

fault, North Qazvin fault, and Damghan fault [2]. Seismic activity of Torud, Ipak and Abdarreh faults to the south of the Alborz mountains were followed by surface faulting [2]. The focal mechanism solution of the September 1, 1962 Buin-Zahra and June 22, 2002 Changureh earthquakes, which occurred on the southward dipping Ipak and Abdarreh faults respectively, indicate predominance of thrust movements. However, field observations suggest that left-lateral movement dominates reverse movement along the Ipak fault [2]. The Khazar fault, a reverse fault with a southward dip direction, is the longest active fault in the Alborz, and is located in the northern edge of the Alborz Mountains. This structure separates the Caspian depression to the north from the Alborz Mountains in the south. The activity of some of the faults within the Alborz mountain range has been documented using historical and recent earthquakes. The Rudbar-Tarom Earthquake of June 20, 1990 was associated with 80 km of discontinuous earthquake faulting [2]. The focal mechanism solution for this earthquake implies a left-lateral strike slip movement on a west-northwest fault plane. The surface faulting also indicates a small reverse component. The preliminary study found no convincing Holocene activity along the 1990 surface ruptures, and no active geomorphological features could be detected on the aerial photographs, or satellite imagery. Based on such evidences, it can be deduced that the earthquakes are not necessarily caused by the reactivating of old or recent faults, but in regions of distributed deformation such as the Iranian plateau, the possibility of formation of new faults in wide active fault zones is conceivable [2].

4. Active Faults of the Studied Region

Consideration of active faults is very important for any seismotectonic study. Based on the available evidences and resources, the length and minimum distances of the active faults in the studied region are presented in Table (1) for 200 km radius of Bojnurd. Figure (3) shows the 26 active faults that are identified in the studied regions which are associated mainly with Kopeh-Dagh and, to a lesser

Table 1. Characteristics of the active faults in a 200 km radius of Bojnurd [12].

Fault Name	Min. Dis. to Center of Bojnurd (km)	Fault Length (km)	Type of Faulting	Maximum Surface Magnitude, M_S (Using Nowroozi, Eq. 1 [13]).
Robat-e Gharbil	29.8	169.47	Strike-Slipe	7.4
Esfarayen	38.1	115.06	Strike-Slipe	7.2
Baghan Garmab	50.45	81.49	Strike-Slipe	7.0
F-4	24.7	100.59	Strike-Slipe	7.1
Neyshabur	142.91	67.85	Strike-Slipe	6.9
Harnestan (F-6)	73.82	257.04	Strike-Slipe	7.6
Jajrum	65.4	76.94	Strike-Slipe	7.0
Ghuchan	82.2	116.8	Strike-Slipe	7.2
Rivand	92.4	71.04	Strike-Slipe	6.9
Joghatai	98.84	75.99	Strike-Slipe	7.0
Keshafroud	162.6	41.19	Thrust-Inverse	6.6
Meyamey	124.75	111.29	Strike-Slipe	7.2
Sabzevar	125.2	84.18	Strike-Slipe	7.0
F-14	123.9	93.72	Strike-Slipe	7.1
F-15	92.31	97.89	Thrust-Inverse	7.1
F-16	113.23	79.46	Thrust-Inverse	7.0
F-17	91.43	134.81	Thrust-Inverse	7.3
F-18	115.51	108.87	Thrust-Inverse	7.2
F-19	101.7	49.95	Strike-Slipe	6.7
Binalud	140.54	65.91	Thrust-Inverse	6.9
F-21	39.41	36.34	Strike-Slipe	6.6
F-22	98.24	34.04	Strike-Slipe	6.5
F-23	111.98	32.25	Strike-Slipe	6.5
F-24	83.48	96.07	Strike-Slipe	7.1
F-25	139.59	33.85	Strike-Slipe	6.5
F-26	164.93	40.58	Strike-Slipe	6.6

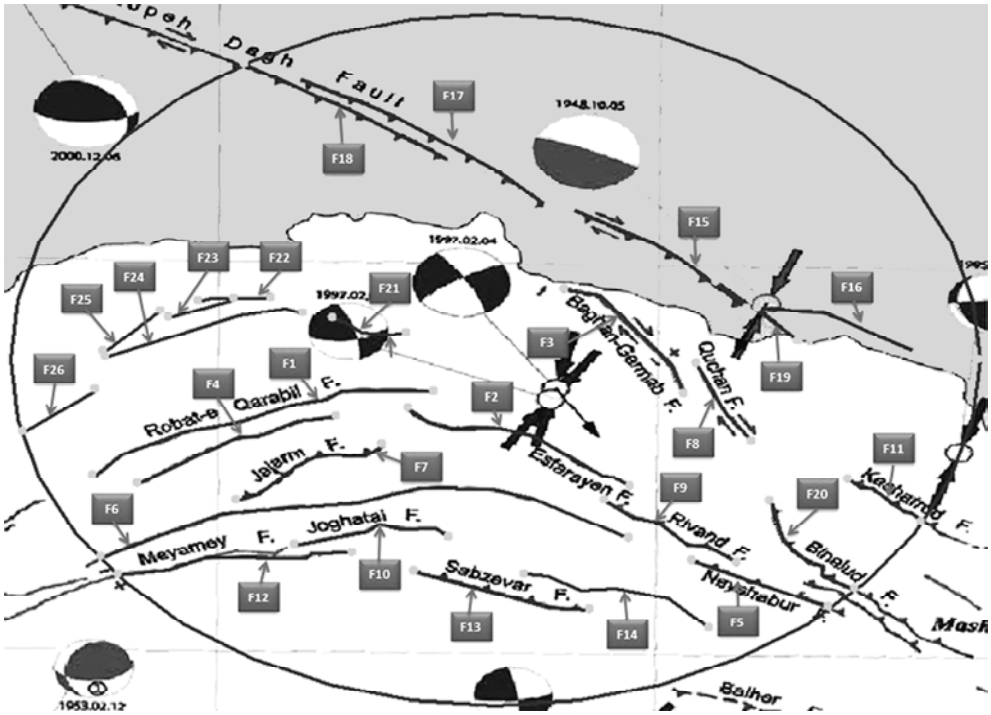

Figure 3. Map of Bojnurd region faults in radius of 200 km [12].

extent, to Alborz belts that influence the seismicity of Bojnurd city. Some of these active faults are: Robat-e Gharbil, Esfarayen, Baghan Garmab, Neyshabur, Harnestan, Jajrum, Ghuchan, Rivand, Joghatai, Keshafroud, Meyamey, Sabzevar, and Binalud. Table (1) also lists the length, the rupture length and the minimum distance of the 26 identified active faults from the center of Bojnurd city. The rupture length of a fault is considered to be 50% of the total fault length.

5. Earthquake Data

Past earthquakes in the studied region can be divided into three categories:

1. Historical earthquakes, before 1900;
2. Inaccurate instrumental earthquakes, which have been recorded since 1900 till 1963, by seismographs;
3. Accurate instrumental earthquakes, which have been recorded from 1964 up to now, using the Wood-Anderson seismographs.

Unfortunately, the information of the historical earthquakes of Bojnurd city is too incomplete. Table (2) lists the available information on the historical earthquakes in the studied region, including their geographical coordinates, year of occurrence, and surface wave magnitudes [12].

According to Iran's International Institute of Earthquake Engineering and Seismology (IIEES) [12], 346 earthquakes are recorded since 1900. After eliminating after- and fore-shocks, the number of earthquakes recorded with $M_S \geq 4.0$ are 175, and $M_S \geq 5$ are 28 records. Moreover, the original catalogs used in this study are attached as a sepa-rate file to this article. Figure (4) presents percentage of the number of earthquakes occurred with respect to their surface wave magnitude,

Table 2. The historical earthquakes in the region [12].

M_S	Latitude	Longitude	Year
7.6	37.6	57.0	943
5.3	36.2	58.8	1145
7.6	36.4	58.7	1209
5.3	36.2	58.8	1251
7.1	36.2	58.8	1270
7.6	36.2	58.8	1389
7.6	36.2	58.8	1405
7.0	36.8	57.0	1695
6.5	38.0	57.2	1810
6.2	37.3	58.1	1833
7.2	37.4	58.4	1871
5.8	37.0	56.2	1883
7.1	37.0	58.4	1893
6.8	37.1	58.4	1895

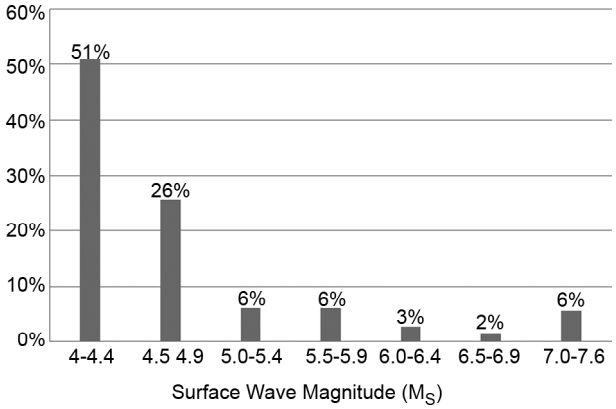

Figure 4. Percentage of surface wave magnitude of the earthquakes in the studied region [12].

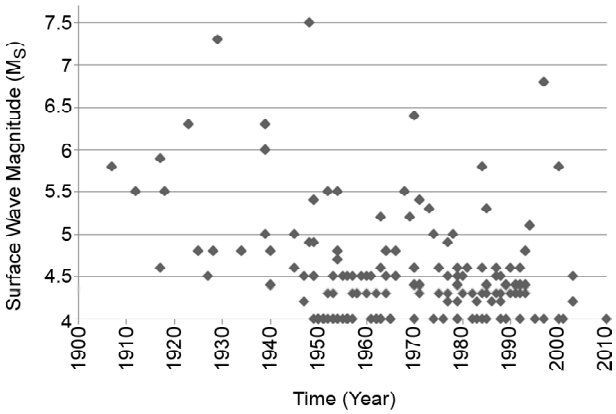

Figure 5. Time distribution of instrumental earthquakes in the studied region [12].

M_S. Figure (5) depicts time distribution of the earthquakes occurred with respect to their surface wave magnitude, M_S. It is clear that most of the earthquakes have magnitudes of less than 4.5 and mostly recorded after 1950.

6. Focal Depth of the Earthquakes

Accurate information is not available about the depth of the ordinary earthquakes. Although focal depths have been reported for many of the occurred earthquakes in the studied region, they are not reliable due to small magnitude of most occurred earthquakes and weak arrangement of stations. According to the information presented in the attached catalog of the earthquakes in the region [12], the main seismic activities (moderate and severe earthquakes) in this region generally have depths smaller than 20 km. The mean depth of the seismic zone in the studied region is considered 8-12 km.

7. The Assessment of Seismic Potential of Faults in Bojnurd City Region

Several methods are usually used to assess seismic potential of faults, which can be divided into two categories. Initial evidences are used to estimate the magnitude of earthquakes in the first category, where the length of surface rupture and maximum displacement are the most common parameters of evidences. Some other parameters like fault rupture or seismic moment are used as well. The second category includes methods that try to assess the magnitude of earthquakes using secondary evidences like liquefaction and landslides. These methods are yet to be developed and experimented. Maximum earthquake magnitude has been assessed by the length of surface rupture in this study.

Nowroozi [13] relationship was used to express the relationship between fault rupture and the earthquake magnitude, see Eq. (1).

$$M_S = 1.259 + 1.244 \times \mathrm{Log}(L_r) \quad (1)$$

where M_S is surface wave magnitude, and L_r is rupture length in meter. The models of faulting used to calculate the maximum magnitude, is based on the assumption of 50% of rupture in fault length during an earthquake. Table (1) provides the maximum surface waves magnitude (M_S), for the active faults in the studied region.

8. The Statistical Specifications of the Seismicity Studies

Seismic hazard parameters relate the earthquake magnitude to the cumulative number of past earthquakes over a given period of time. Gutenberg and Richter [17] relation, Log $N = a - bM$, is one of such relationships, where N is the number of past earthquakes with magnitude M over a given period of time, and b is seismicity coefficient of a region. Gutenberg and Richter [17] relation can also be written as $\mathrm{Ln}\,\lambda = \alpha - \beta M$ in which $\alpha = a\,\mathrm{Ln}\,10$, $\beta = b\,\mathrm{Ln}\,10$, and $\lambda = (N/t)$. The seismic hazard parameters this way are: maximum expected magnitude of a region (M_{max}), annual activity rate (λ) and seismicity coefficient of region (β). They describe numerical quantities of a statistical model for any given region. In order to assess these quantities, the seismic speci-

fications of past earthquakes in that region should be studied and their effects on the site need to be calculated. Therefore, it is essential to gather earthquake data and analyze them statistically. These data are received from seismological stations and used for the analysis. The information that these data include are: date and time of occurrence, coordination of epicenter, magnitude, focal depth and the reporting center. There are some differences in determined parameters reported by different sources. The differences are due to the complicated specifications of earthquakes and possible errors in measurements of stations.

Earthquake magnitude is one of the important parameters to analyze and predict the strong ground motion. In fact, the strength of an earthquake is assessed by magnitude scales. This parameter is estimated from the peak wave amplitude which is recorded by seismograms. Different types of magnitudes are defined considering type and period of waves and also distance from the epicenter. This is indicated by the magnitude sign, M, and different subscripts. Since all magnitudes reported for historical earthquakes are in the form of surface wave, also instrumental earthquakes are based on surface wave, or volumetric wave, then, the magnitude of the surface wave, M_S, is used for all data. Using the relationship, see Eq. (2), presented by Iranian Committee of Large Dams (IRCOLD 1994) [14], the magnitude based on the volumetric wave, m_b is converted into M_S:

$$M_S = 1.2\, m_b - 1.29 \qquad (2)$$

where the magnitudes are different from M_S or m_b, for example in the form of M_L (local magnitude), and M_w (moment magnitude) one may use Table (3) to interrelate (interpolate) those magnitudes to surface wave magnitude [15].

Table 3. Correlation between different types of magnitudes [15].

M_S	M_W	M_L
3.6	4.5	4.8
4.6	5.2	5.3
5.6	5.8	5.8
6.6	6.6	6.3
7.3	7.3	6.8

9. Elimination of the Foreshocks and After Shocks

In seismic hazard analysis of a region, it is assumed that occurred earthquakes are location and time independents. It means that earthquakes occur successively in space and time along faults or in seismic regions. Therefore, the occurrence time of an upcoming earthquake is independent of the last earthquake.

Regarding the mentioned limitations, foreshocks and aftershocks that are related to principal earthquakes should be eliminated from the database. The most common method to eliminate aftershocks and foreshocks is to consider the time and location windows for their occurrences. Therefore in order to detach aftershocks and foreshocks from principal earthquakes and eliminate them from Catalogue, Gardner and Knopoff [16] method is used. The criteria for the eliminations are:

- Their magnitudes must be less than the magnitude of the principal earthquake (M).
- The distance between epicenters of these earthquakes from the principal earthquake must be less than $S(M)$.
- Time differences between these earthquakes and the principal earthquake should not be more than $T(M)$. $S(M)$ and $T(M)$ are experimental parameters. Table (4) lists the time and location windows for elimination of aftershocks and foreshocks by Gardner and Knopoff method [16].

10. Time Distribution of Peak Earthquake Magnitudes

In order to conduct a probabilistic seismic hazard study, the earthquake catalogue in a 200 km region

Table 4. Time and location windows for elimination of aftershocks and foreshocks by Gardner and Knopoff method [16].

Magnitude (M_S)	Distance (km)	Time (day)
4	30	42
4.5	35	83
5	40	155
5.5	47	290
6	54	510
6.5	61	790
7	70	915
7.5	81	960
8	94	985

encircling Bojnurd has been gathered and processed to eliminate aftershocks and foreshocks. According to historical earthquakes in the region, the most severe earthquake occurred in years of 943, 1389 and 1405 with a magnitude of 7.6. Furthermore, on October 5, 1948, the highest instrumental earthquake was recorded in the studied region with a magnitude of 7.3 in the form of body wave (m_b) [17]. Figure (6) illustrates the location of occurred historical and instrumental earthquakes in 200 km radius of Bojnurd city.

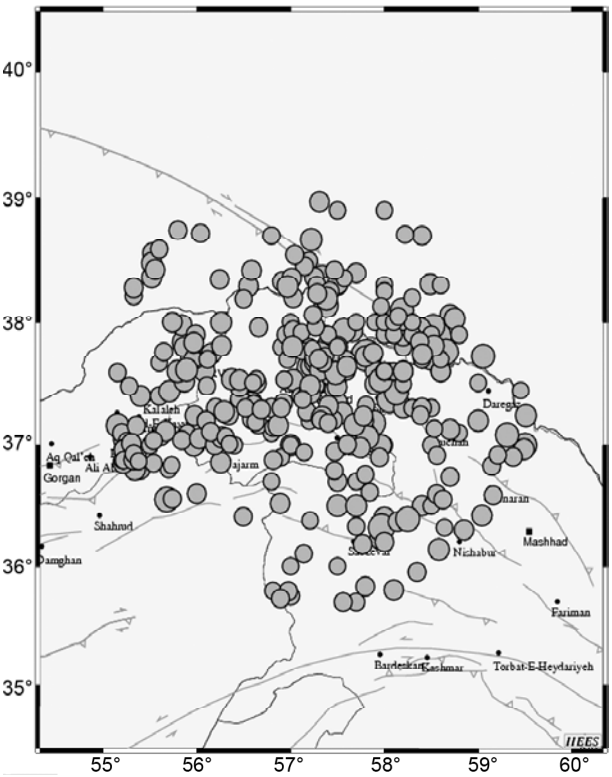

Figure 6. The distribution of earthquake epicenters in the studied region [12].

11. Assessment of Earthquake Hazard Parameters

The seismic hazard coefficients of the region (value of the Gutenberg and Richter [17] relation) have been evaluated using maximum likelihood method [18]. Besides, the return period and the occurrence probability of each magnitude have also been calculated by the Kijko [19] software.

Different methods are used in assessment of seismic hazard parameters. Selection of the proper method is done on the basis of engineering judgment, reliability of the seismic data and uncertainties in their report. Generally, recorded earthquakes of any region in Iran only represent a part of occurred earthquakes in the region, and many earthquakes are never recorded. Some reasons of insufficiency of earthquake data in Iran can be expressed as follows. In the case of historical earthquakes, historians might have not recorded some earthquakes or some records might have been ruined, or in some cases they might have been ignorant of some earthquakes because of the distance. And in the case of instrumental earthquakes, lack of seismographs was the main reason. The accuracy of recorded data also varies. Thus historical earthquakes are more uncertain and instrumental earthquakes, which occurred in recent years are more accurate. Therefore, Kijko [19] method is used to calculate the seismic hazard parameters. The method has the ability to analyze earthquake data of different accuracy.

In this study, the minimum magnitude (M_{min}) is 4.0 in the form of surface waves (M_S). Kijko method is based on double truncated Gutenberg-Richter distribution function and the Maximum Likelihood estimation method.

In this paper, three different categories of earthquakes are taken into consideration:

1. Historical earthquakes (before 1900) with the magnitude error of 0.5 (the first time period);
2. Inaccurate instrumental earthquakes (1900-1963) with the magnitude error of 0.2 (the 2nd time period);
3. Accurate instrumental earthquakes (1964-2006) with the magnitude error of 0.1 (the 3rd time period).

The calculation results of seismic hazard parameters from all historical and instrumental earthquakes by using Kijko method are as follows:

$\beta = 2.05 \pm 0.08$ ($b = 0.89 \pm 0.04$)

$\lambda = 1.15 \pm 0.1$ (for $M_{min} = 4.00$)

$M_{max} = 8.10 \pm 0.64$

12. Return Period Analysis of Earthquakes

After calculating the seismic hazard parameters, the return periods of earthquakes in the studied region are calculated and plotted against the surface wave magnitude, M_S in Figure (7) for Bojnurd city and its vicinity. According to this analysis, an e arthquake with a return period of 100 years has a

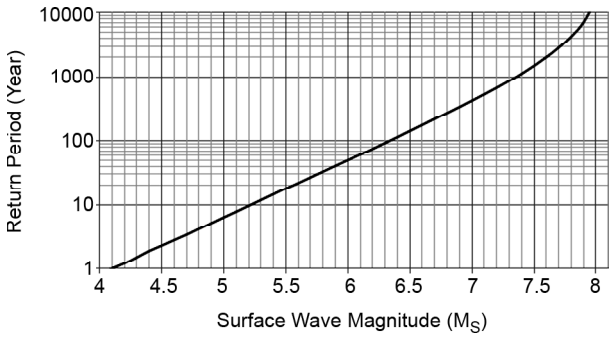

Figure 7. The relationship between the return period and the magnitude by using Kijko method.

magnitude of 6.4, and with return periods of 475 and 2475 years the magnitudes are about 7.1, and 7.7, respectively.

13. Strong Ground Motion Parameters in the Region of Bojnurd City

Different parameters are involved in ground motion. These parameters include the peak velocity, the peak acceleration, the maximum displacement and other parameters which are present in the frequency content of the records. Seismic design codes, however, mostly use the peak horizontal ground acceleration (PGA) and Uniform Hazard Spectra (UHS) as two index parameters representing the nature of the strong ground motion. Both parameters are highly dependent to the earthquake magnitude, epicenter distance and geological specifications. Modern seismic codes prefer to use UHS, as the maximum response of a single degree of freedom system with a given period, subjected to all earthquakes with different source mechanism, but having the same probability of occurrence. This research is to assess the PGA and UHS over the bedrock by probabilistic seismic hazard analyses. PGA is represented by, *A*, in Iranian Code of Practice for Seismic Resistant Design of Buildings [9] that is used to directly calculate the base shear exerted to the buildings by the earthquake. UHS is not currently adopted by Std. 2800, however, following the Seismic Rehabilitation Code for Existing Buildings [20], it is common among the researchers to compare 70% of the elastic design spectrum of Std. 2800 with UHS corresponding to 10% risk in 50 years and 150% of the elastic design spectrum of Std. 2800 with UHS corresponding to 2% risk in 50 years.

14. Basic Steps in Probabilistic Assessment of Earthquake Hazard Parameters

The steps involved in assessing hazard parameters (such as PGA or UHS) for an ideal "bedrock" condition can be summarized as follows:

1) Modeling of seismic sources;
2) Evaluation of recurrence relationship;
3) Evaluation of attenuation relationship for hazard parameters;
4) Estimation of activity rate for probable earthquakes;
5) Evaluation of basic parameters such as maximum magnitude [21-22].

Numerous seismic hazard forecasting models were developed within the last several decades. The simplest widely used model is the Poisson model with the assumptions that seismic events are spatially and temporally independent and the probability that two seismic events will take place at the same location and at the same time approaches zero [23].

It was mentioned earlier that the occurrence relationship of Gutenberg and Richter and Poisson model are used as the function of the probability prediction of the earthquake occurrence in the future.

15. Seismic Sources Model in the Region of Bojnurd City

There are different ideas to select seismic sources model. The point sources model is not very accurate because of the uncertainty in the location of the earthquakes and inadequate data of past earthquakes. In the case of the regional sources model, there isn't enough information about different regions in Iran. Consequently, assuming the same seismicity parameters, the model of linear sources is used, and it is also assumed that the seismic power of all the active faults in the region is equal.

16. Selection of the Proper Attenuation Relationships

Attenuation relationships are the most important elements in the seismic hazard analysis which represent the relationship between peak seismic hazard parameters, the distance from the surface epicenter of the earthquake and the magnitude. Selection of the most proper model among the various attenuation models of the strong ground motion is done based on following criteria:

- The relationship can be applicable for the studied region.
- The distance of the site or sites from the seismic sources must be in the determined maximum and minimum range of the relationship.
- The earthquake magnitude scale of the region is the same as the magnitude scale in the relationship.
- The maximum and minimum values of earthquake magnitudes in the region are the same as the magnitudes from relationship.
- The focal depth of earthquakes of the region must be in the range of the attenuation relationship.
- The soil type of the studied region and the attenu ation relationship must be the same.
- The mechanism of the most seismic sources of the studied region must be the same as the mechanism of the attenuation relationship.

In this study, after assessing different attenuation relationships for derivation of PGAs, according to the above-mentioned conditions, three attenuation relationships of Ghodrati et al [22], Ramazi [24], and Campbell [25] are used with logic tree coefficients of 0.45, 0.30 and 0.25, respectively.

As Ghodrati et al [22], and Ramazi [24] relationships are merely for Iran, then they are considered to be more accurate for the calculation of the strong ground motion in Iran. Consequently, higher weighted coefficient is given to them. However, the highest weighted coefficient is given to Ghodrati et al [22] because it is recent. For computation of UHS, three attenuation relationships of Ghodrati et al [26], Ambarseys [27], and Campbell [25] are used with logic tree coefficient of 0.4, 0.35 and 0.25, respectively. Figure (8) illustrates the logic trees for obtaining PGA and UHS for Bojnurd for different hazard levels.

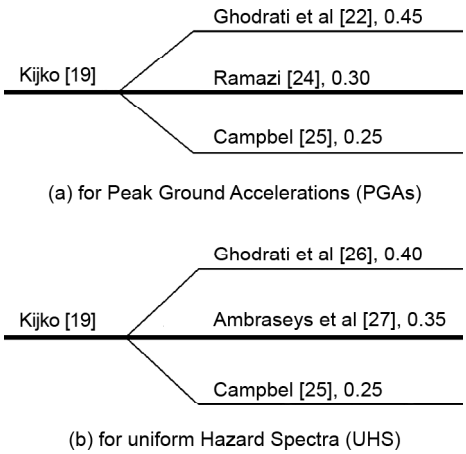

Figure 8. Logic tree coefficients used in calculations.

17. Results and Discussion

In this Research, Bojnurd city and its vicinity is subdivided into a grid of 8×11, total of 88 sites, with 8 vertical and 11 horizontal lines. Probabilistic seismic hazard analysis is then carried out for each site. In order to analyze the seismic hazard regarding the region faults, the seismic sources of the region are modeled and with the required parameters for the seismotectonic model, the seismicity parameters, PGAs and UHS have been calculated for each of attenuation relationships, and then introduced separately to SEISRISK III [28]. The program outputs are mixed by logic tree coefficients as shown in Figure (8). Then final results, as PGAs and UHS over the bedrock are calculated for 88 sites of Bojnurd city, see Figure (9), based on 10% and 2% probability of being exceeded in 50 years or the return periods of 475 and 2475 years respectively. These hazard levels are introduced in the Seismic Rehabilitation Code for Existing Buildings [20].

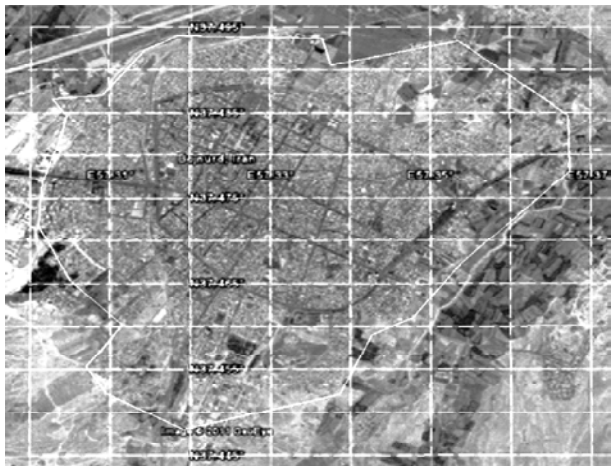

Figure 9. Map Bojnurd region subdivided by 8 vertical and 11 horizontal lines (88 sites).

Iso-acceleration zoning maps of PGA of Bojnurd city for each hazard level are represented in Figure (10). Figures show that the northern parts of Bojnurd city have the highest PGAs and iso-acceleration lines are E-W and parallel. Figures (11) to (16) illustrate iso-response acceleration zoning maps of UHS for two different hazard levels of 10% and 2% risks at periods of 0.1, 0.2, 0.3, 0.5, 1.0 and 2.0 seconds, respectively. Similar to the PGAs, iso-acceleration

lines for UHS are also E-W and increasing toward the north. These lines for hazard level 2 and for higher periods in some parts of the region may seem disorderly, which can be attributed to the selected proximity of the 88 sites/points. In fact, if there were fewer numbers of points with farther distances, the same E-W trend would have been observed for those parts as well.

A comparison of the calculated values in this study in the return period of 475 years with the proposed design acceleration of the Iranian Code of Practice for Seismic Resistant Design of Buildings

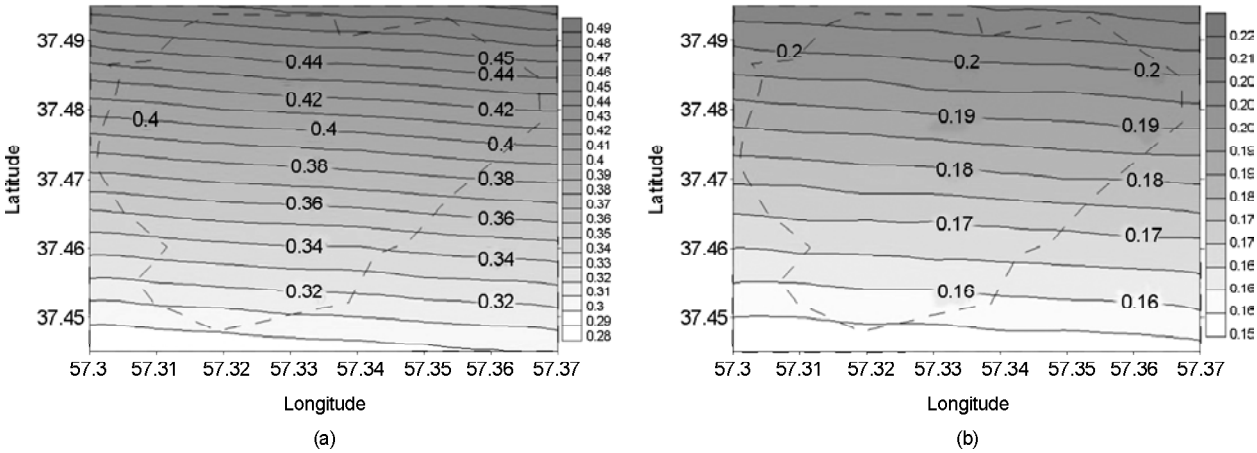

Figure 10. Map of PGA over bedrock for Bojnurd a) 2%, and b) 10% risks of being exceeded in 50 years.

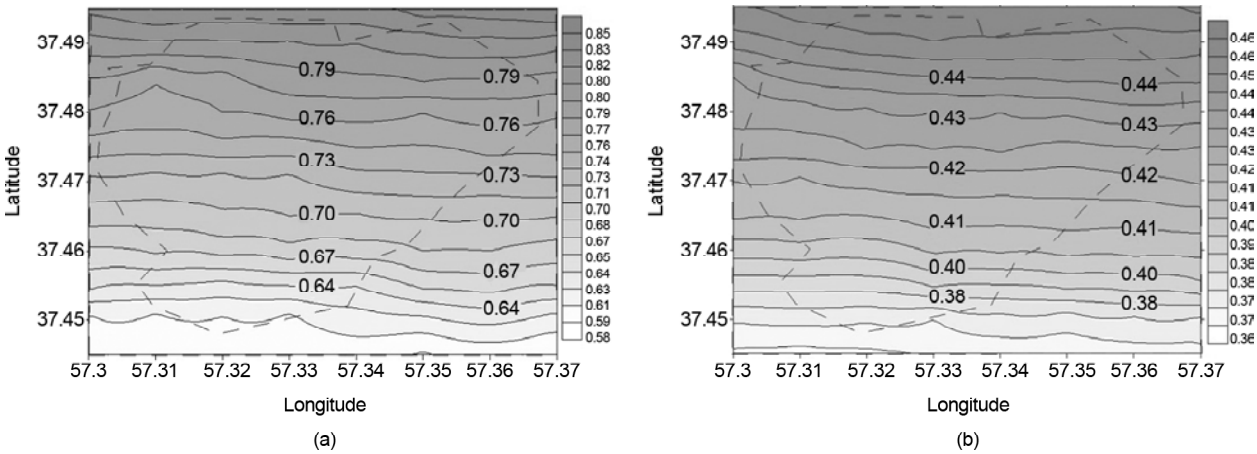

Figure 11. Map of UHS (For T=0.1 s) over bedrock for Bojnurd a) 2%, and b) 10% risks of being exceeded in 50 years.

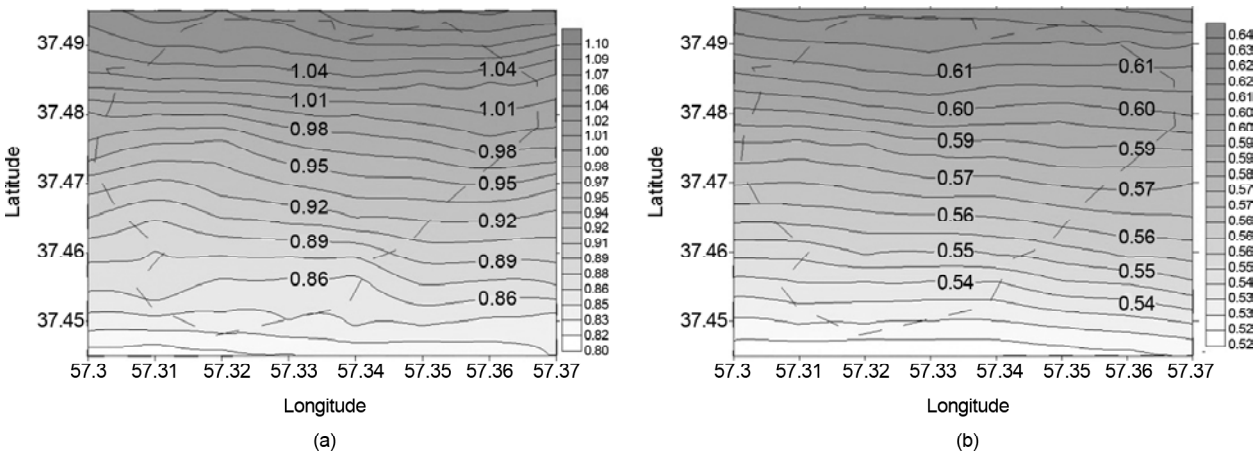

Figure 12. Map of UHS (For T=0.2 s) over bedrock for Bojnurd a) 2%, and b) 10% risks of being exceeded in 50 years.

(BHRC 2005) shows that the proposed values of the Std. 2800 (A = 0.3 g) are in the safe side even in the northern parts of the city. But, this study is for a limited region with its special conditions. However, the PGAs obtained are more precise for the studied region.

The main contribution of this research is intended to be the derivation of site specific UHS and PGA zoning maps for different hazard levels for the first time for the city of Bojnurd. The city of Bojnurd by recently becoming the capital of North Khorasan province, and its potential for a rapid future expan-

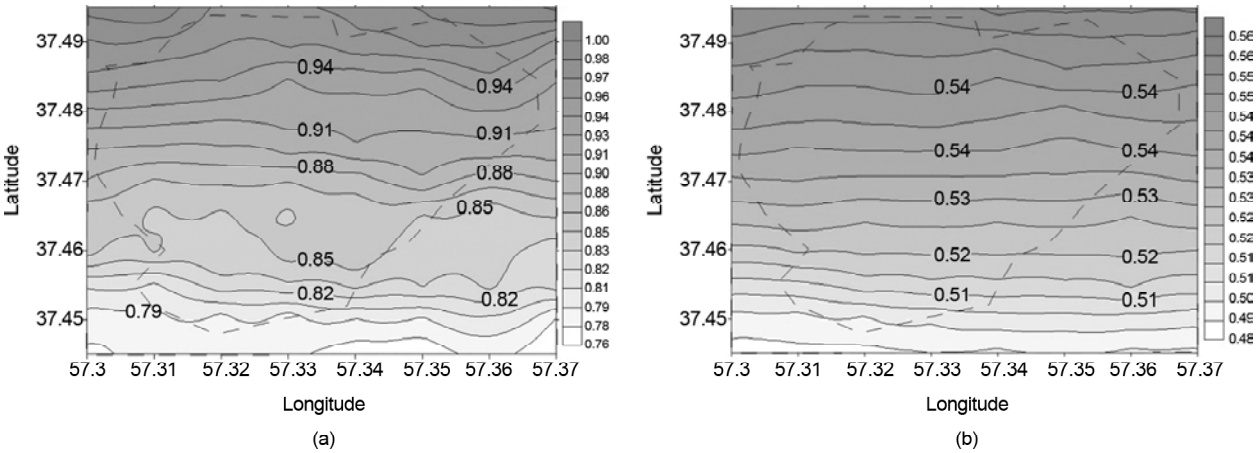

Figure 13. Map of UHS (For T=0.3 s) over bedrock for Bojnurd a) 2%, and b) 10% risks of being exceeded in 50 years.

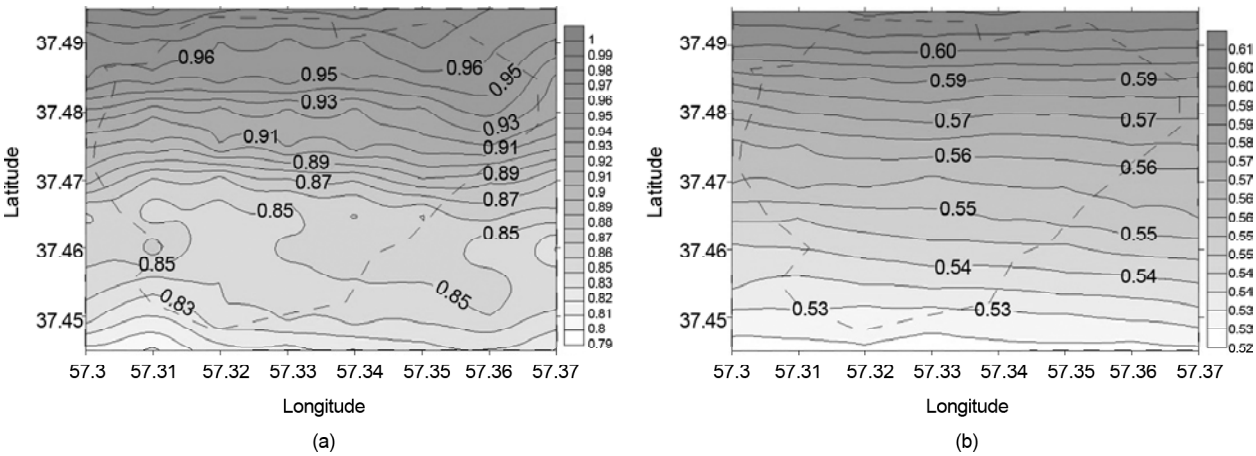

Figure 14. Map of UHS (For T=0.5 s) over bedrock for Bojnurd a) 2%, and b)10% risks of being exceeded in 50 years.

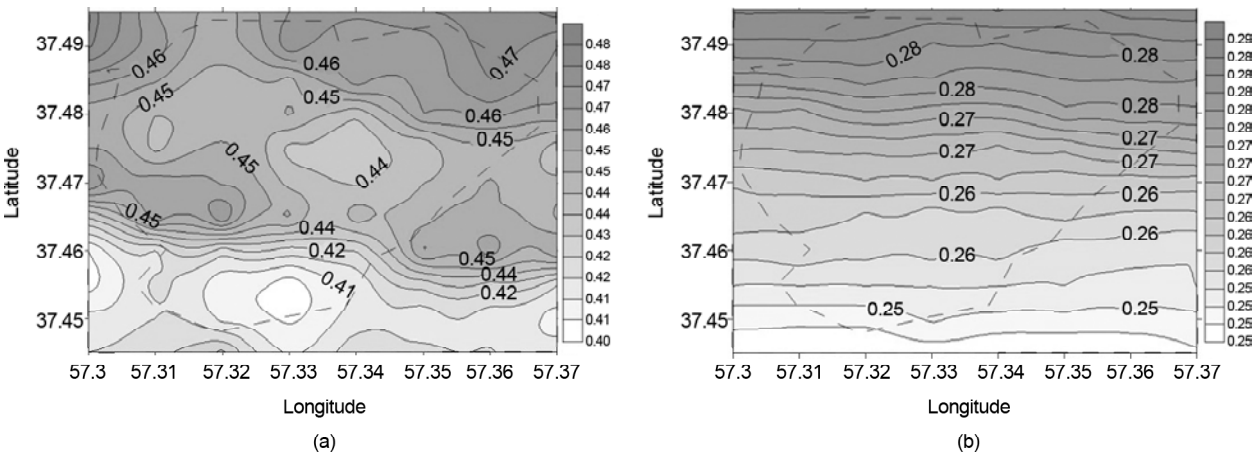

Figure 15. Map of UHS (For T=1.0 s) over bedrock for Bojnurd a) 2%, and b) 10% risks of being exceeded in 50 years.

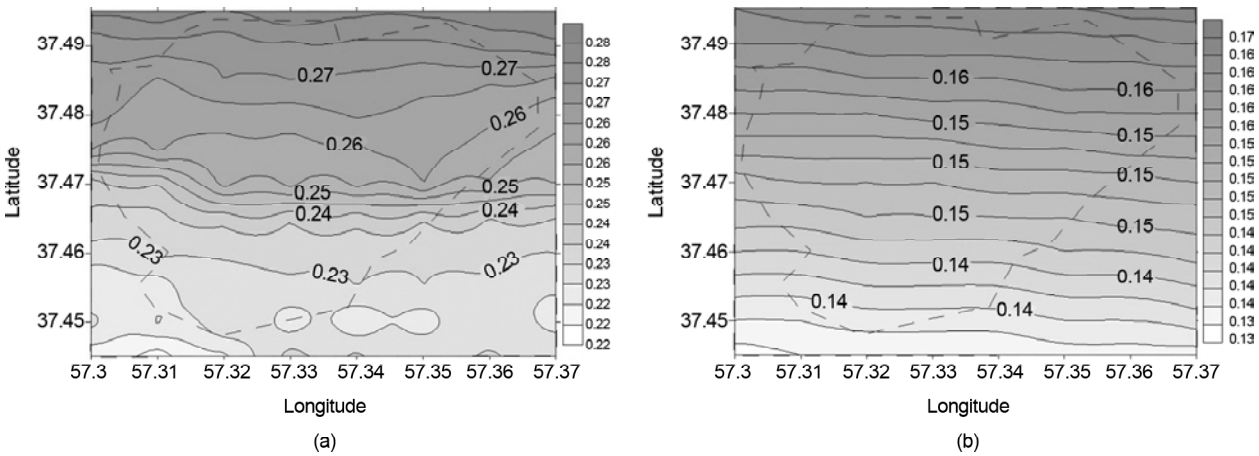

Figure 16. Map of UHS (For T=2.0 s) over bedrock for Bojnurd a) 2%, and b) 10% risks of being exceeded in 50 years.

sion is in great need of the outcome of such researches. The latest available information on different probabilistic assessment methodologies, attenuation relationships, and seismic source zones in the region, etc. has led to a more realistic assessment of the seismic risks in the studied region. In fact, Iran's seismic code authorities have now higher responsibility to expand such studies for the entire country.

Despite Iran's Std. 2800 which only provides a constant PGA of 0.3g for the entire region and only for hazard level 1, this research provides site specific PGAs and UHS for 88 different sites and for two hazard levels of 1 and 2, see Figures (10) to (16).

The use of 88 different sites in the city and the seismic source zones in an area encircling a radius of 200 km from the city center is justified by the fact that the city of Bojnurd has recently become the capital of North Khorasan and its potential for a rapid expansion in future demands such a detailed study.

The site specific PGAs and UHS obtained in this study are at bedrock level. In order to determine these quantities at ground surface (on the basin), a site/soil amplification study must be conducted for different sites in the region. Therefore, the soil profiles for these 88 different sites must be obtained. In addition, such study requires earthquake ground motion records which represent the seismicity of the region. The outcome of such a research, although essential, is beyond the scope of this current work.

18. Conclusions

In this study, zoning maps of the peak horizontal ground acceleration (PGA) and uniform hazard spectra (UHS) over the bedrock in different parts of Bojnurd city are presented for two hazard levels 10%, and 2% probability of being exceeded during life cycles of 50 years, see Figures (10) to (16). The minimum and maximum values of PGA for hazard levels 1 and 2 are obtained as (0.15, 0.22) and (0.28, 0.49), respectively. For hazard level 1, Iran's Std. 2800 specifies a design PGA of A = 0.3g which is less than 0.22g obtained here. The minimum and maximum values of UHS for hazard level 1 at periods of 0.1, 0.2, 0.3, 0.5, 1.0, and 2.0 seconds are (0.36, 0.46), (0.52, 0.64), (0.48, 0.56), (0.52, 0.61), (0.25, 0.29), and (0.13, 0.17), respectively. The minimum and maximum values of UHS for hazard level 2 at periods of 0.1, 0.2, 0.3, 0.5, 1.0, and 2.0 seconds are (0.58, 0.85), (0.80, 1.10), (0.78, 1.00), (0.79, 1.00), (0.40, 0.48), and (0.22, 0.28), respectively.

The results also show that the northern part of Bojnurd city has the highest, and southern part has the least amount of PGA and UHS.

Figure (17) provides a comparison of minimum, mean, and maximum Uniform Hazard Spectra (UHS-min, UHS-mean, and UHS-max respectively) with seismic design spectra from Iran's Std. 2800 for the studied region for 10%, and 2% risks of being exceeded in 50 years. For a given hazard level, and a given period, UHS-min and UHS-max are the least and the highest UHS values, respectively, of the entire 88 points in the studied region, and UHS-mean is the mean value of all the 88 UHS values. According to this figure, for hazard level 1, for long period range ($\geq$ 0.6 to 0.7 s) all the UHS are less than the spectra corresponding to 70% of that of Std. 2800, and in the short period range the UHS-

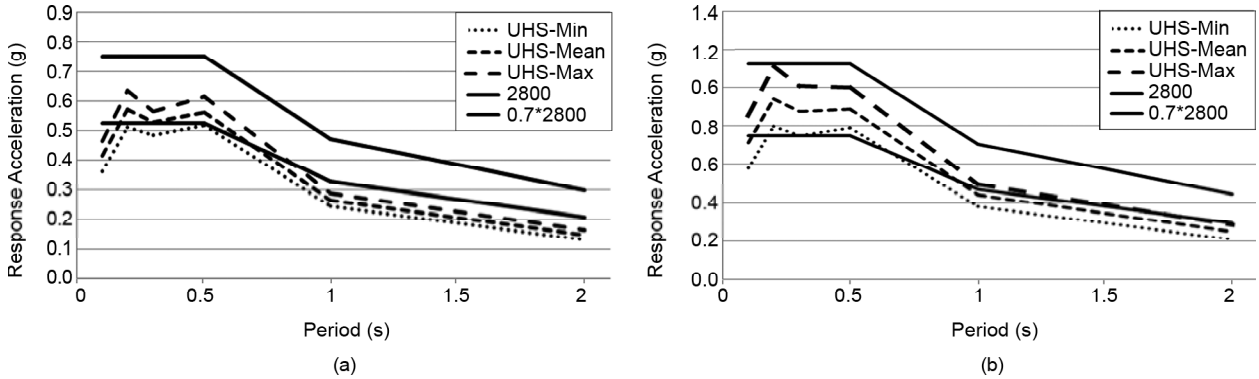

Figure 17. Comparison of minimum, average, and maximum Uniform Hazard Spectra (UHS) with seismic design spectra from Iran's Std. 2800 for the studied region for a) 10%, and b) 2% risks of being exceeded in 50 years.

mean is about the same as 70% of Std. 2800 spectrum, and the maximum spectra exceeds from the 70% of Std. 2800 but still less than the Std. 2800's spectrum. This indicates that the elastic design forces by Std. 2800 for hazard level 1 are acceptable. For hazard level 2, similar to hazard level 1, for long period range ($\geq$ 0.6 to 0.7 s) all the UHS are close or slightly less than the spectrum corresponding Std. 2800, and in the short period range the UHS-mean and UHS-max exceed the Std. 2800's design spectrum but still less than the 150% of Std. 2800's spectrum.

References

1. Wikipedia, the Free Encyclopedia (2011). http://en.wikipedia.org/wiki/Bojnurd.

2. Hessami, K. and Jamali, F. (2006). Explanatory Notes to the Map of Major Active Faults, *Journal of Seismology and Earthquake Engineering*, **8**(1), 1-16.

3. Heidarzadeh, M., Pirooza, M.D., Zaker, N.H., Yalciner, A.C., Mokhtari, M., and Esmaeily, A. (2008). Historical Tsunami in the Makran Subduction Zone off the Southern Coasts of Iran and Pakistan and Results of Numerical Modeling, *Ocean Engineering*, **35**, 774-786.

4. Tavakoli, B. (1996). Major Seismotectonic Provinces of Iran, International Institute of Earthquake Engineering and Seismology, Internal Document.

5. Tavakoli, B. and Ghafory-Ashtiany, M. (1999). Seismic Hazard Assessment of Iran, International Institute of Earthquake Engineering and Seismology (IIEES).

6. Berberian, M. (1995). Master 'blind' thrust fault Hidden under the Zagros Folds: Active Basement Tectonics and Surface Morphotectonics, *Tectonophysics*, **241**, 193-224.

7. Newmark, N.M., and Hall, W.J. (1982). Earthquake spectra and design, Earthquake Engineering Research Institute, Berkeley, Calif.

8. Humar, J.L. and Rahgozar, M.A. (1996). Application of Inelastic Response Spectra Derived from Seismic Hazard Spectral Ordinates for Canada, *Canadian Journal of Civil Engineering*, **23**(5), 1051-1063.

9. Building & Housing Research Center (BHRC) (2005). Iranian Code of Practice for Seismic Resistant Design of Buildings, Publication PNS-253, 3rd Revision, 135 (http://www.bhrc.ir).

10. Stocklin, J. (I968). Structural History and Tectonics of Iran: a Review, *Bull. Am. Assoc. Petrol. Geol.*, **52**(7), 1229-1258.

11. Tchalenko, J.S. (1975). Seismicity and Structure of the Kopeh-Dagh (Iran, U.S.S.R.), Philosophical Transactions of the Royal Society of London, Series A, Mathematical and Physical Sciences, **278**(1275), 1-28.

12. International Institute of Earthquake Engineering and Seismology (IIEES), http://www.iiees.ac.ir.

13. Nowroozi, A. (1985). Empirical Relations between Magnitude and Fault Parameters for Earthquakes in Iran, *Bull. Seismol. Soc. Am.*, **75**(5), 1327-1338.

14. IRCOLD, Iranian Committee of Large Dams (1994). Relationship between M_s and m_b, Internal Report (In Persian).

15. Ghodrati Amiri, G., Motamed, R., and Es-Haghi, H.R. (2003). Seismic Hazard Assessment of Metropolitan Tehran, Iran, *J. Earthq. Eng.*, **7**(3), 347-372.

16. Gardner, J.K. and Knopoff, L. (1974). Is the Sequence of Earthquake in Southern California, with Aftershocks Removed, Poissonian, *Bull. Seismol. Soc. Am.*, **64**(5), 1363-1367.

17. Gutenberg, B. and Richter, C.F. (1954). Seismicity of the Earth and Associated Phenomena, Princeton University Press, New Jersey.

18. Kijko, A. and Sellevoll, M.A. (1992). Estimation of Earthquake Hazard Parameters from Incomplete Data Files, Part II, Incorporation of Magnitude Heterogeneity, *Bull. Seismol. Soc. Am.*, **82**(1), 120-134.

19. Kijko, A. (2000). Statistical Estimation of Maximum Regional Earthquake Magnitude M_{max}, *Workshop of Seismicity Modeling in Seismic Hazard Mapping*, Poljce, Slovenia, Geol. Surve, 1-10.

20. American Society of Civil Engineers (2007). ASCE 41-06, Seismic Rehabilitation of Existing Buildings.

21. Abdalla, J.A., Mohamedzein, Y.E.-A., and Abdel Wahab, A. (2001). Probabilistic Seismic Hazard Assessment of Sudan and Its Vicinity", *Earthquake Spectra*, **17**(3), 399-415.

22. GhodratiAmiri, G., Mahdavian, A., and Manouchehri Dana, F. (2007). Attenuation Relationships for Iran, *J. Earthq. Eng.*, **11**(4), 469-492.

23. Kayabali, K. (2002). Modeling of Seismic Hazard for Turkey Using the Recent Neotectonic Data, *Eng. Geol.*, **63**, 221-232.

24. Ramazi, H.R. (1999). Attenuation Laws of Iranian Earthquakes, *Proceedings of the 3rd International Conference on Seismology and Earthquake Engineering*, Tehran, Iran, 337-344.

25. Campbell, K.W. (1997). Empirical Near-Source Attenuation Relationships for Horizontal and Vertical Components of Peak Ground Acceleration, Peak Ground Velocity, and Pseudo-Absolute Acceleration Response Spectra, *Seismological Research Letters*, **68**(1), 154-179

26. Ghodrati Amiri, G., Khorasani, M., Mirza Hesabi, R., and Razavian Amrei, S.A.(2010). Ground-Motion Prediction Equations of Spectral Ordinates and Arias Intensity for Iran, *J. of Earthquake Engineering*, **14**(1), 1-29.

27. Ambraseys, N.N., Simpson, K.A., and Bommer, J.J. (1996). Prediction of Horizontal Response Spectra in Europe, Earthquake Engineering and Structural Dynamics, **25**, 371-400.

28. Bender, B. and Perkins, D.M. (1987). SEISRISK-III: A Computer Program for Seismic Hazard Estimation, US Geol. Survey Bull., 1772.